Journal of Radiotherapy in Practice

Journal of Radiotherapy in Practice (2011)
10, 261–271

doi:10.1017/S1460396910000427

Original Article

Monte Carlo study on mucosal dose in oral and nasal cavity using photon beams with small field

James C.L. Chow[1,2,3], Amir M. Owrangi[1]

[1]*Department of Radiation Physics, Princess Margaret Hospital,* [2]*Department of Radiation Oncology, University of Toronto, Toronto, Ontario, Canada,* [3]*Department of Physics, Ryerson University, Toronto, Ontario, Canada*

Abstract

We study how mucosal dose in the oral or nasal cavity depends on the irradiated small segmental photon fields varying with beam energy, beam angle and mucosa thickness. Dose ratio (mucosal dose with bone underneath to dose at the same point without bone) reflecting the dose enhancement due to the bone backscatter was determined by Monte Carlo simulation (EGSnrc-based code), validated by measurements. Phase space files based on the 6 and 18 MV photon beams with small field size of 1×1 cm^2, produced by a Varian 21 EX linear accelerator, were generated using the BEAMnrc Monte Carlo code. Mucosa phantoms (mucosa thickness = 1, 2 and 3 mm) with and without a bone under the mucosa were irradiated by photon beams with gantry angles varying from 0 to 30°. Doses along the central beam axis in the mucosa and the dose ratio were calculated with different mucosa thicknesses. For the 6 MV photon beams, the dose at the mucosa-bone interface increased by 44.9–41.7%, when the mucosa thickness increased from 1 to 3 mm for the beam angle ranging from 0 to 30°. These values were lower than those (58.8–53.6%) for the 18 MV photon beams with the same beam angle range. For both the 6 and 18 MV photon beams, depth doses in the mucosa were found to increase with an increase of the beam angle. Moreover, the dose gradient in the mucosa was greater for the 18 MV photon beams compared to the 6 MV. For the dose ratio, it was found that the dose enhancement due to the bone backscatter increased with a decrease of mucosa thickness, and was more significant at both the air-mucosa and mucosa-bone interface. Mucosal dose with bone was investigated by Monte Carlo simulations with different experimental configurations, and was found vary with the beam energy, beam angle and mucosa thickness for a small segmental photon field. The dosimetric information in this study should be considered when searching for an optimized treatment strategy to minimize the mucosal complications in the head-and-neck intensity-modulated radiation therapy.

Keywords

Mucosal dose; Monte Carlo; inhomogeneities; head-and-neck IMRT

INTRODUCTION

In head-and-neck radiation therapy, the goal is to deliver a highly conformal dose to a prescribed target volume while sparing surrounding healthy tissue as much as possible.[1,2] However, this cannot be easily achieved because of complications that arise with existing treatment planning methods such as intensity-modulated radiation therapy (IMRT) as a clinical consequence of the radiation dose to the mucosa.[3–6] When a patient is treated for

Correspondence to: James C.L. Chow, Department of Radiation Physics, Princess Margaret Hospital, Toronto, Ontario, M5G 2M9 Canada. E-mail: james.chow@rmp.uhn.on.ca

head-and-neck cancer with IMRT, the mucosa are irradiated by very small segmental photon beams with field sizes of about 0.25–1 cm^2. This may result in acute complications including oropharyngeal mucositis, xerostomia and sialadenitis, and chronic complications including mucosal fibrosis, xerostomia caries, tissue necrosis and cutaneous fibrosis.[4–6] It is found that the mucosa becomes thicker in the oral or nasal cavity due to complication in the course of radiation therapy.[5,6]

In order to reduce mucosal complications, a reliable method is needed to calculate the mucosal dose in the course of treatment planning. This is difficult because the tumours are mostly small, irregular, inhomogeneous structures usually located at or close to an air-tissue-bone or air-tissue interface.[7–9] The determination of the energy deposition in such complex structures is especially challenging for the small segmental mega-voltage (MV) photon fields used in radiation therapy. Commercial semi-empirical/analytic dose calculation algorithms such as the pencil beam and convolution/supervision methods depend on the assumption of transient charge particle equilibrium,[10,11] which is difficult to achieve on a short length scale due to the increased lateral electron path in air.[12–14] Moreover, the thickness of the head-and-neck mucosal layer is on the millimeter scale. To determine the deposited energy with sufficient accuracy the resolution of the calculation should be at least one order of magnitude smaller than that of the object (i.e., on the 0.1 mm length scale). Current commercial treatment planning software is difficult to support dose calculations at 0.1 mm resolution for the head-and-neck IMRT plan.[15]

Monte Carlo simulation is independent on the assumption of charge particle equilibrium and therefore has the potential to yield much higher accuracy than current commercial algorithms for the dose deposited by small segmental photon fields.[16–19] Moreover, the Monte Carlo method is well established as a means of predicting the dose deposited in inhomogeneous systems involving tissue, air and bone.[20–22] Monte Carlo simulations using EGSnrc-based codes are a possible way to predict the absorbed dose within small, highly irregular inhomogeneous structures such as the mucosa in the oral cavity.

In this study, 6 and 18 MV photon beams with small field size of 1×1 cm^2, which suffer from lateral electronic disequilibrium in a homogeneous medium, were used to irradiate a thin layer of mucosa tissue with different thicknesses (1–3 mm). The mucosa was on top of a bone slab to mimic the oral or nasal cavity in head-and-neck radiation therapy. By varying the photon beam energy, beam angle and mucosa thickness, dose in mucosa (with bone underneath) was compared to that in normal tissue (without bone), so that the effect of bone backscatter on the mucosal dose can be investigated.

MATERIALS AND METHODS

Experimental configuration

The simulation geometry of the mucosa phantom with bone can be found in Figure 1. 6 and 18 MV photon beams with field size of 1×1 cm^2, produced by a Varian 21 EX linear accelerator, were used to irradiate a phantom containing a 5 cm bone slab with a layer of mucosa on top. The mucosa thickness was varied from 1 to 3 mm and the source-to-surface distance (SSD) of the photon beam was equal to 90 cm. Apart from setting the photon beam angle to zero, the beam was rotated 3, 5, 10, 20 and 30° clockwise with the source-to-axis distance equal to 100 cm. Doses along the central beam axis (CAX) in the mucosa were calculated by Monte Carlo simulations using the EGSnrc-based code with different beam energies and geometries. To study the dose enhancement due to the bone backscatter in the mucosa, another phantom with the bone slab replaced by the tissue was used with all the above dose calculations repeated. A dose ratio in the mucosa phantom with and without the bone slab was determined with different beam energies and geometries.

Monte Carlo simulation

The Electron Gamma Shower (EGSnrc) code version 4-r2-3-0 developed by the National

https://doi.org/10.1017/S1460396910000427 Published online by Cambridge University Press

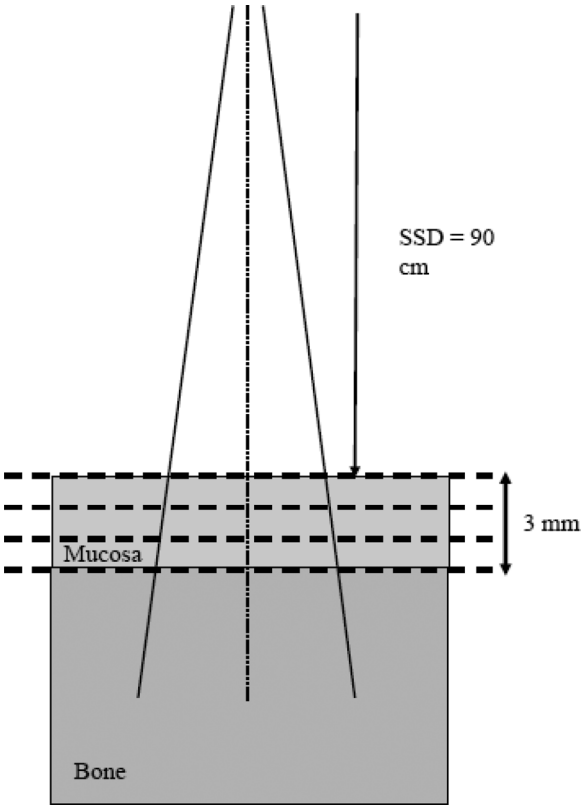

Figure 1. Schematic diagram (not to scale) showing the beam geometry and experimental configuration used in Monte Carlo simulations. 6 and 18 MV photon beams with field size of 1 × 1 cm^2 were used. The thickness of the bone slab was equal to 5 cm.

Research Council Canada was used in this study.[23,24] The code was run on a personal computer with a single INTEL Core2 Quad processor with 2.4 GHz using 3 GB of RAM. BEAMnrc and DOSXYZnrc associated with EGSnrc were used to generate the phase space files with the small segmental photon fields and calculate the dose.[25–27]

Modeling of photon beams with small field size

Phase space files containing the particle information such as its type (electron, position or photon), incident angle and energy from a scoring plane, based on a Varian 21 EX linear accelerator, were generated for the 6 and 18 MV photon beams. The description of the linear accelerator including the geometries and materials of different components in the gantry head was provided by the manufacturer. The field size of both files was set to 1 × 1 cm^2 and each file contained 5 million particles. The EGSnrc-based BEAMnrc code was used to generate the phase space files with transport parameters of the electron cut-off energy (ECUT) = 700 keV, photon cut-off energy (PCUT) = 10 keV and maximum fractional electron energy loss per step (ESTEPE) = 0.25.[26] The Parameter Reduced Electron Step Transport Algorithm II (PRESTA II) was used as the electron-step algorithm.[28] The user-adjustable parameters for the above algorithm were set at their default values. The radius of the input electron beam was set to 2 mm and the energy of the beam was chosen to be the nominal acceleration potential of the photon beam. Detailed description of how to determine the nominal acceleration potential of the photon beam can be found in our previous work.[29] The above phase space files were used to calculate doses in the mucosa phantom as shown in Figure 1.

Validations of the Monte Carlo phase space models were carried out using the scanning water tank system (RFA 300, Scanditronix Medical AB) and photon diode (Scanditronix Medical AB, PDF-3G). The servo motor system of the water tank was controlled by the Omni Pro 6 software for the required sampling resolution. The photon diode was used for the small field measurement because of its small active sampling area and thickness of 2 mm and 60 μm, respectively.[30]

Dose calculation

Doses along the CAX in the phantom with and without bone (Figure 1) were calculated using the DOSXYZnrc code with the phase space files generated in the previous section.[27] The voxel size in the phantom was set to 2 × 2 × 0.1 mm^3 corresponding to the x (cross-line), y (in-line) and z (along the CAX) axis. Dose calculations were carried out according to the experimental configuration in Figure 1. The mucosa thickness was set to 1, 2 and 3 mm with the beam angle varying from 0 to 30°. Doses in both mucosa phantoms with and without bone were calculated with the number of histories equal to 20 million. Using this number of histories, the relative dose error (uncertainty as a fraction of dose in the voxel) was found

https://doi.org/10.1017/S1460396910000427 Published online by Cambridge University Press

to be around 1% based on the Monte Carlo output files.[27] ICRPBONE700ICRU and ICRUTISSUE700ICRU were selected as the bone and mucosa tissue materials in simulations. The transport parameters of the ECUT, PCUT and ESTEPE in DOSXYZnrc were set to 700 keV, 10 keV and 25%, respectively.

RESULTS

The percentage depth doses (PDDs) and beam profiles were determined by measurements and Monte Carlo simulations for the 6 and 18 MV photon beams. Figure 2a,b shows the PDDs and beam profiles for the 6 MV photon beams, respectively, while Figure 2c,d shows the PDDs and beam profiles for the 18 MV photon beams. The SSD was set to 90 cm and beam profiles were measured at a depth of 10 cm. It can be seen that both the PDDs and beam profiles determined by measurements and Monte Carlo simulations agreed well. Therefore, phase space files of the 6 and 18 MV photon beams with field size of 1×1 cm^2 were verified.

The depth doses in the mucosa varied with different thicknesses of 1, 2 and 3 mm were shown in Figure 3a–c for the 6 MV photon beams, respectively. Beam angles of 0, 10, 20 and 30° were used in the phantoms with and without bone under the mucosa. Figure 4a–c has the same experimental configurations as Figure 3a–c except the photon beam energy was changed from 6 to 18 MV. The dependences of the mucosal dose on the beam angle with different mucosa thicknesses of 1, 2 and 3 mm were shown in Figure 5a–c for the 6 MV photon beams. Doses at different depths in the phantoms with and without bone were shown in Figure 5. Figure 6a–c has the same experimental configurations as Figure 5a–c except the energy of the photon beam was changed to 18 MV. Dose ratios (dose at a point in the

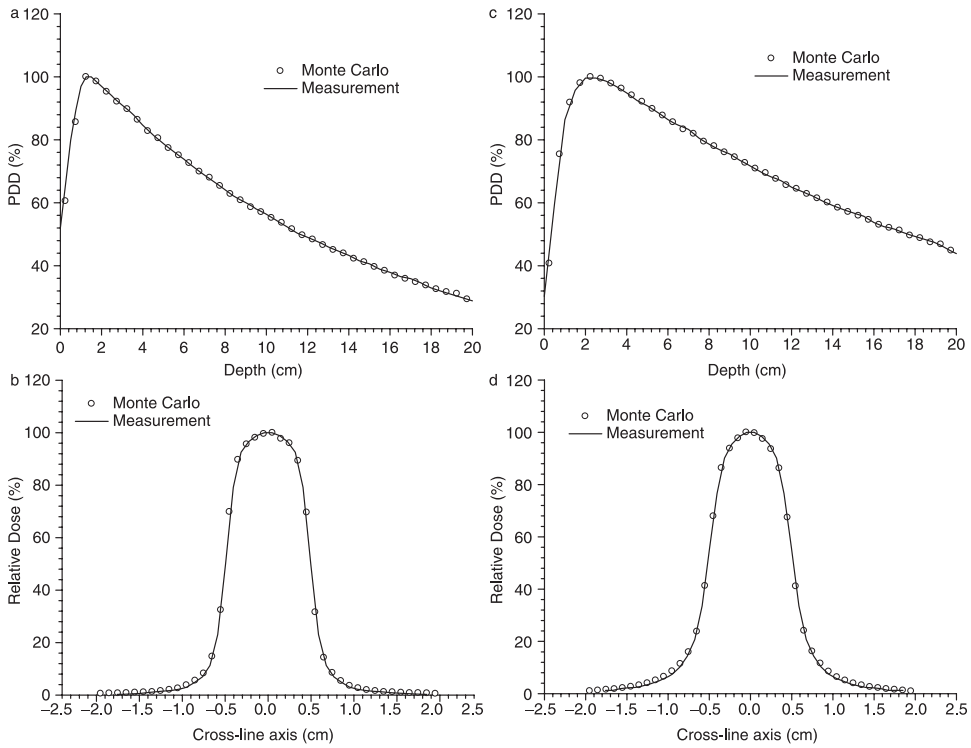

Figure 2. (a,b) The percentage depth doses and beam profiles for the 6 MV photon beams with field size of 1×1 cm^2, respectively. (c,d) The percentage depth doses and beam profiles for the 18 MV photon beams. Doses were measured and calculated by photon diode and Monte Carlo simulation with SSD = 90 cm. The beam profiles were determined at a depth of 10 cm.

https://doi.org/10.1017/S1460396910000427 Published online by Cambridge University Press

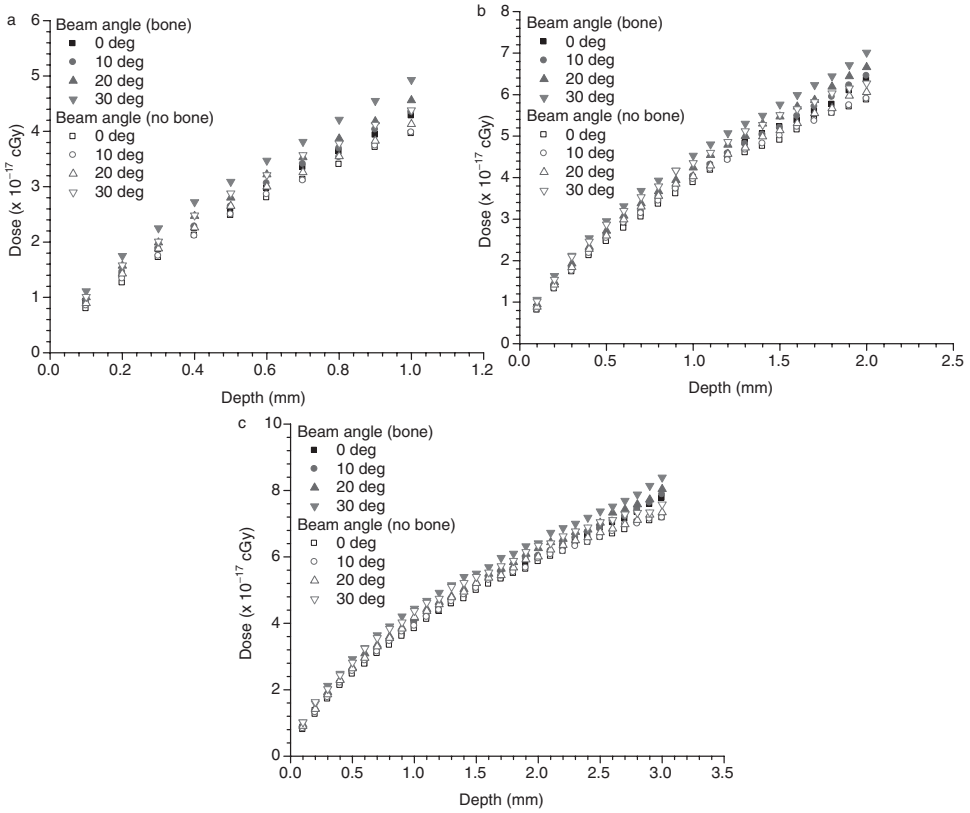

Figure 3. Depth doses in the mucosa with thicknesses of (a) 1, (b) 2 and (c) 3 mm varying with beam angles of 0, 10, 20 and 30° using the 6 MV photon beams.

mucosa phantom with the bone slab to dose at the same point in the phantom with the bone slab replaced by tissue) were determined with different mucosa thicknesses and beam geometries. Dose ratios with different beam angles (0, 3, 5, 10, 20 and 30°) varying with mucosa thicknesses of 1, 2, and 3 mm for the 6 MV photon beams were shown in Table 1(a–c). Table 2(a–c) has the same experimental configurations as Table 1(a–c) except the photon beam energy was 18 MV.

DISCUSSION

Depth dependence on mucosal dose

In Figure 3, it is seen that the depth dose in the mucosa is larger in the phantom with the bone slab (Figure 1) than the phantom without the bone slab. This dose enhancement particularly at the mucosa-bone interface is due to the bone backscatter. For the 6 MV photon beams, it is found that the dose (maximum) at the mucosa-bone interface increases from 4.3–4.9 to 7.8–8.4 $\times$ 10^{-17} cGy with the mucosa thickness increases from 1 to 3 mm for beam angle varying from 0 to 30°. This shows that for beam angle between 0 and 30°, an increase of the mucosal dose by 44.9–41.7% is found when the mucosa becomes thicker during the course of treatment. When the 18 MV photon beams are used, the maximum mucosal dose at the mucosa-bone interface increases from 11.3 (0°)–14.2 (30°) to 27.4 (0°)–30.6 (30°) $\times$ 10^{-17} cGy with the mucosa thickness increases from 1 to 3 mm, as shown in Figure 4. This means that an increase of mucosal dose by 58.8–53.6% can be found within a beam angle range of 0–30°, when the mucosa thickness increases from 1 to 3 mm. The larger maximum mucosal dose for the 18 MV than 6 MV

https://doi.org/10.1017/S1460396910000427 Published online by Cambridge University Press

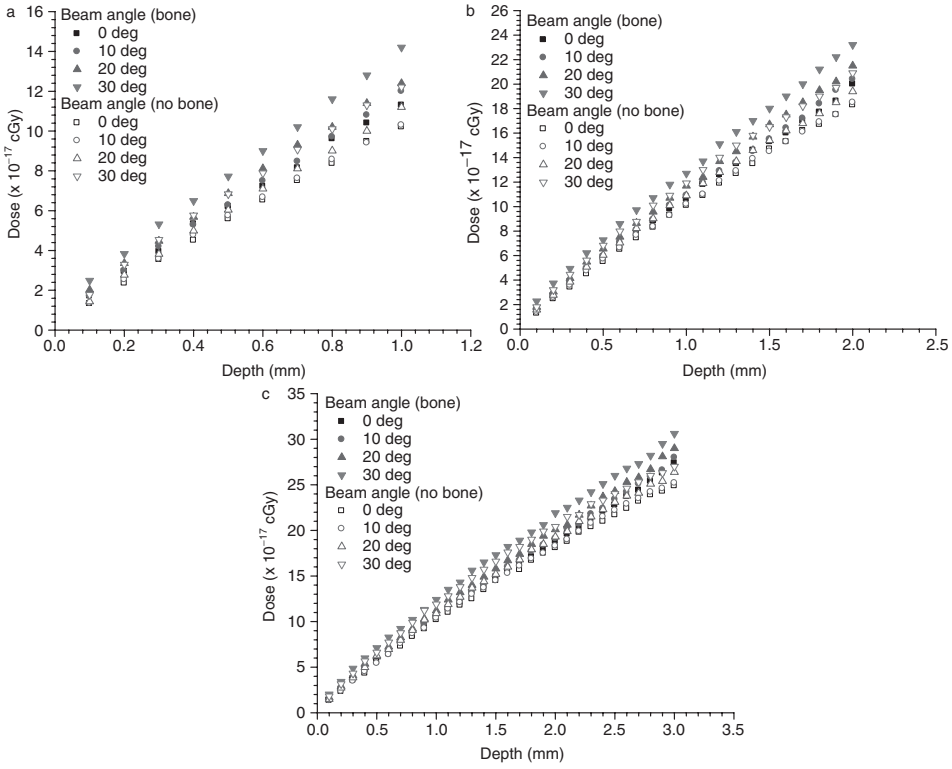

Figure 4. Depth doses in the mucosa with thicknesses of (a) 1, (b) 2 and (c) 3 mm varying with beam angles of 0, 10, 20 and 30° using the 18 MV photon beams.

photon beams is due to the larger mucosal surface dose for the 18 MV beams as seen in Figures 3 and 4. However, it should be noted that the percentage surface dose for the 6 MV photon beam is larger than that of the 18 MV, when the dose is normalized to the dose at the depth of maximum dose (d_{max}) as shown in Figure 2a,c.

The difference between the depth doses with and without bone in the mucosa phantom shows the dose enhancement due to the bone backscatter. In Figures 3 and 4, it can be seen that the dose enhancement in the mucosa is largest at the mucosa-bone interface and decreases toward the mucosa surface. This is due to the attenuation of the backscattered dose from the mucosa-bone interface to the surface. This dose enhancement can be interpreted using the dose ratio which defined as the dose in the mucosa with the bone underneath to that without. Relationship between the dose ratio and the photon beam energy, beam angle, mucosa thickness and depth can be found in the following sections in details. For 1 mm thickness of mucosa and beam angle equal to zero, the dose gradient of the 18 MV photon beams is 2.8 times greater than that of the 6 MV. For thicker mucosa of 2 and 3 mm, dose gradients of the 18 MV beams are 3.5 and 3.8 times greater than those of the 6 MV. It can be seen that the dose gradient increases with the mucosa thickness and the dose distribution in the mucosa is more sensitive to the 18 MV photon beams than the lower energy.

Both the depth doses for the 6 and 18 MV photon beams are affected by the beam angle. It can be seen in Figures 3 and 4 that depth doses increase with the beam angle for both the mucosa phantoms with and without bone. The increase of surface dose due to the beam obliquity can be explained by the pencil beam model of overlapping the tilted ''tear-drop'' shaped pencil beam dose volume, and can be found elsewhere.[31,32] More detailed discussion

https://doi.org/10.1017/S1460396910000427 Published online by Cambridge University Press

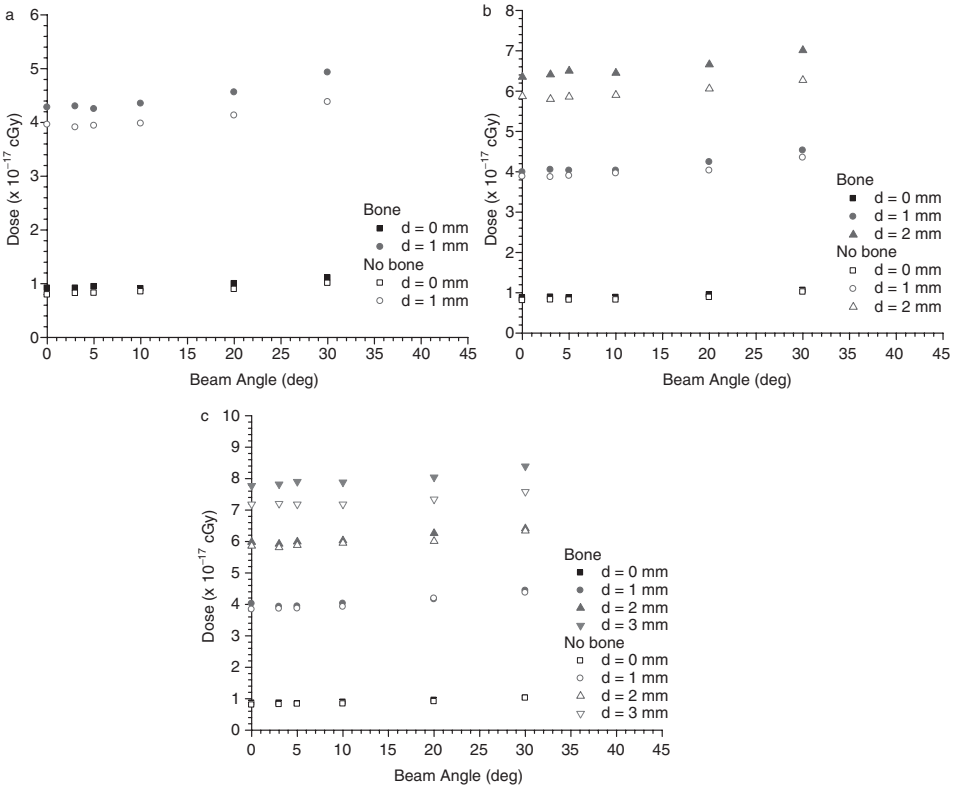

Figure 5. Relationship between dose and beam angle at different depths in the mucosa with thicknesses of (a) 1, (b) 2 and (c) 3 mm using the 6 MV photon beams.

in the relationship between the mucosal dose and beam angle can be found in the next section.

Beam angle dependence on mucosal dose

The relationship between doses at different depths and beam angle can be seen in Figures 5 (6 MV) and 6 (18 MV). In Figure 5, doses at different depths only increase slightly with an increase of the beam angle, and doses in the mucosa with bone are larger than those without. When the depth is greater or closer to the mucosa-bone interface, the dose increases due to the presence of the bone backscatter. On the other hand, the dose enhancement due to the bone backscatter can be seen by comparing doses in the mucosa with and without bone. In Figures 5 and 6, the difference between doses with and without bone is always larger for the depth closer to the mucosa-bone interface. For the 18 MV photon beams (Figure 6), doses at different depths increase only slightly (same as the 6 MV beam). However, both photon beam energies show a larger extent of dose increase when the depth is greater. It means that the closer the depth to the mucosa-bone interface, the larger the sensitivity of the dose dependence on the beam angle.

Dose ratio and mucosa thickness

Dose ratios mentioned above, reflecting the dose enhancement due to the bone backscatter, are shown in Tables 1 and 2 for the 6 and 18 MV photon beams. It should be noted that the dose ratio considers the dose point at the same position with and without the bone under the mucosa. For a photon beam with a fixed beam angle, both point doses with and without the bone suffer from the same effect of dose enhancement due to the beam obliquity. Therefore, the effect of beam angle does not reflect on the dose ratio. In Table 1(a) for a relatively thin layer of mucosa (1 mm), the dose

https://doi.org/10.1017/S1460396910000427 Published online by Cambridge University Press

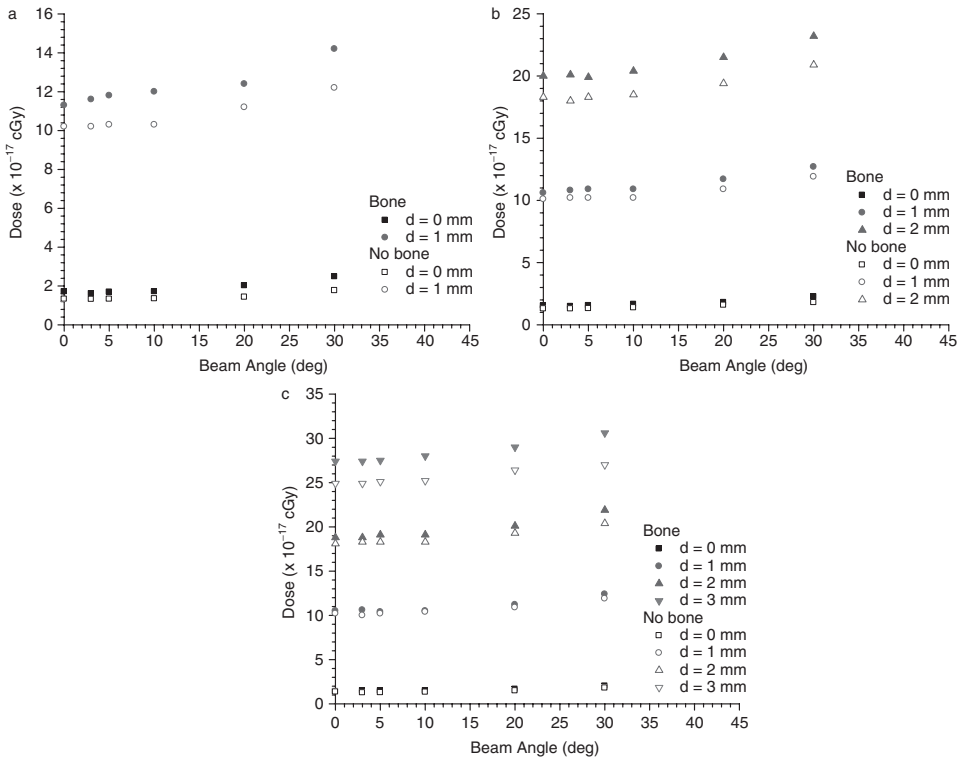

Figure 6. Relationship between dose and beam angle at different depths in the mucosa with thicknesses of (a) 1, (b) 2 and (c) 3 mm using the 18 MV photon beams.

Table 1. *Tables showing dose ratios of mucosa with to without bone for the 6 MV photon beams varying with depth and beam angle with mucosa thicknesses of (a) 1, (b) 2 and (c) 3 mm*

	Beam angle (°)					
	0	**3**	**5**	**10**	**20**	**30**
(a) 1 mm						
0 mm	1.15	1.11	1.14	1.07	1.12	1.09
1 mm	1.08	1.09	1.08	1.09	1.10	1.13
(b) 2 mm						
0 mm	1.08	1.08	1.07	1.07	1.07	1.04
1 mm	1.03	1.05	1.03	1.02	1.05	1.04
2 mm	1.08	1.11	1.11	1.09	1.10	1.12
(c) 3 mm						
0 mm	1.07	1.05	1.01	1.06	1.04	1.01
1 mm	1.05	1.02	1.02	1.03	1.00	1.02
2 mm	1.02	1.02	1.02	1.01	1.04	1.01
3 mm	1.08	1.09	1.10	1.10	1.10	1.11

enhancement is between 8 and 15% for the beam angle ranging from 0 to 30°. This is different from thicker mucosa (2 mm and 3 mm), which have lower dose enhancement ranging from 3 to 12% and 1 to 11%, respectively. It can be seen that the dose enhancement increases with decrease of the mucosa thickness. Higher dose enhancement can be found for the 18 MV photon beams with thicknesses equal to 1 mm (11–40%), 2 mm (5–27%) and 3 mm

https://doi.org/10.1017/S1460396910000427 Published online by Cambridge University Press

Table 2. *Tables showing dose ratios of mucosa with to without bone for the 18 MV photon beams varying with depth and beam angle with mucosa thicknesses of (a) 1, (b) 2 and (c) 3 mm*

	Beam angle (°)					
	0	**3**	**5**	**10**	**20**	**30**
(a) 1 mm						
0 mm	1.29	1.22	1.27	1.27	1.41	1.40
1 mm	1.11	1.14	1.15	1.17	1.11	1.16
(b) 2 mm						
0 mm	1.18	1.15	1.18	1.20	1.14	1.27
1 mm	1.05	1.06	1.07	1.07	1.07	1.07
2 mm	1.09	1.12	1.09	1.10	1.11	1.11
(c) 3 mm						
0 mm	1.04	1.18	1.15	1.11	1.11	1.12
1 mm	1.03	1.06	1.02	1.01	1.03	1.04
2 mm	1.04	1.03	1.04	1.04	1.04	1.08
3 mm	1.10	1.10	1.10	1.11	1.10	1.13

(3−18%) for the beam angle range of 0−30°. This higher dose ratio is due to the larger surface dose for the 18 MV photon beams than that for the 6 MV.

In Table 1(b), it is found that the dose ratios are larger at both the air-mucosa (1.04−1.08) and mucosa-bone interface (1.08−1.12) than the middle position (1.02−1.05) in the mucosa. This dosimetric issue is also true for Table 1(c). For 3 mm thickness of mucosa, the dose ratios at the air-mucosa (1.01−1.07) and mucosa-bone (1.08−1.11) interface are larger than those in the middle of the mucosa (1.01−1.05). The lower dose ratio or dose enhancement in the middle of the mucosa is due to attenuations of the bone backscatter from the mucosa-bone interface, and of the surface dose from the air-mucosa interface. It is seen in Table 2(b,c) that this effect is more significant in the 18 MV photon beams. This is because of the relatively larger depth dose gradient in the mucosa compared to the 6 MV photon beams.

CONCLUSIONS

Dependences of mucosal dose on the beam energy, beam angle and mucosa thickness for the 6 and 18 MV photon beams with small field size of 1×1 cm^2 were studied by Monte Carlo simulations using the EGSnrc-based code. Depth doses in the mucosa with different thicknesses on top of a bone were calculated. Dose ratios (dose in the mucosa with the bone underneath to dose at the same point without the bone) were determined by calculating doses in the mucosa phantoms with and without a bone slab. For the beam angle ranging from 0 to 30°, mucosal doses increased by 44.9−41.7% and 58.8−53.6% were found when the mucosa was growing thick for the 6 and 18 MV photon beams, respectively. The mucosal dose gradients for the 18 MV photon beams were 2.8, 3.5 and 3.8 times greater than those of the 6 MV photon beams for the 1, 2 and 3 mm thickness of mucosa. Moreover, the mucosal dose was found to increase with the beam angle, and the dose ratio, reflecting the dose enhancement due to the bone backscatter, increased with decrease of the mucosa thickness. It was found that the dose enhancement was larger at both the air-mucosa and mucosa-bone interface than other positions in the mucosa. This is due to the attenuations of the bone backscatter and surface dose. This study provides information of mucosal dose irradiated by small segmental photon fields with various beam energy, beam angle and mucosa thickness. The dosimetric information here should be considered in studying the mucosal complications in head-and-neck IMRT, so that an optimized treatment strategy to minimize mucosal complications can be developed.

https://doi.org/10.1017/S1460396910000427 Published online by Cambridge University Press

ACKNOWLEDGEMENTS

This study was supported by grant from the University of Toronto Dean's Fund. Measurements related to the Monte Carlo validation were carried out in the Grand River Hospital. J.C.L.C would like to thank Varti Vartanian and Mitch Spiegel of Varian Medical Systems for providing detailed information of the 21 EX linear accelerator.

References

1. Jereczek-Fossa BA, Krengli M, Orecchia R. Particle beam radiotherapy for head and neck tumors: radiobiological basis and clinical experience. Head Neck 2006; 28:750–760.
2. Lee N, Puri DR, Blanco AI, Chao KS. Intensity-modulated radiation therapy in head and neck cancers: an update. Head Neck 2007; 29:387–400.
3. Ostwald PM, Kron T, Hamilton CS. Assessment of mucosal underdosing in larynx irradiation. Int J Radiat Oncol Biol Phys 1996; 36:181–187.
4. Franzmann EJ, Lundy DS, Abitbol AA, Goodwin WJ. Complete hypopharyngeal obstruction by mucosal adhesions: a complication of intensive chemoradiation for advanced head and neck cancer. Head Neck 2006; 28:663–670.
5. Scully C, Epstein J, Sonis S. Oral mucositis: a challenging complication of radiotherapy, chemotherapy, and radiochemotherapy: part 1, pathogenesis and prophylaxis of mucositis. Head Neck 2003; 25:1057–1070.
6. Scully C, Epstein J, Sonis S. Oral mucositis: a challenging complication of radiotherapy, chemotherapy, and radiochemotherapy. Part 2: diagnosis and management of mucositis. Head Neck 2004; 26:77–84.
7. Klein EE, Chin LM, Rice RK, Mijnheer BJ. The influence of air cavities on interface doses for photon beams. Int J Radiat Oncol Biol Phys 1993; 27:419–427.
8. Beach JL, Mendiondo MS, Mendiondo OA. A comparison of air-cavity inhomogeneity effects for cobalt-60, 6-, and 10-MV x-ray beams. Med Phys 1987; 14:140–144.
9. Kan WK, Wu PM, Leung HT, Lo TC, Chung CW, Kwong DL, Sham ST. The effect of the nasopharyngeal air cavity on x-ray interface doses. Phys Med Biol 1998; 43:529–537.
10. Davidson SE, Ibbott GS, Prado KL, Dong L, Liao Z, Followill DS. Accuracy of two heterogeneity dose calculation algorithms for IMRT in treatment plans designed using an anthropomorphic thorax phantom. Med Phys 2007; 34:1850–1857.
11. Gagné IM, Zavgorodni S. Evaluation of the analytical anisotropic algorithm in an extreme water-lung interface phantom using Monte Carlo dose calculations. J Appl Clin Med Phys 2007; 8:33–46.
12. Larsson E, Jönsson BA, Jönsson L, Ljungberg M, Strand SE. Dosimetry calculations on a tissue level by using the MCNP4c2 Monte Carlo code. Cancer Biother Radiopharm 2005; 20:85–91.
13. Epp ER, Boyer AL, Doppke KP. Underdosing of lesions resulting from lack of electronic equilibrium in upper respiratory air cavities irradiated by 10MV x-ray beams. Int J Radiat Oncol Biol Phys 1977; 2:613–619.
14. Arnfield MR, Siantar CH, Siebers J, Garmon P, Cox L, Mohan R. The impact of electron transport on the accuracy of computed dose. Med Phys 2000; 27:1266–1274.
15. Starkschall G, Steadham RE Jr, Popple RA, Ahmad S, Rosen II. Beam-commissioning methodology for a three-dimensional convolution/superposition photon dose algorithm. J Appl Clin Med Phys 2000; 1:8–27.
16. De Vlamynck K, Palmans H, Verhaegen F, De Wagter C, De Neve W, Thierens H. Dose measurements compared with Monte Carlo simulations of narrow 6 MV multileaf collimator shaped photon beams. Med Phys 1999; 26:1874–1882.
17. Jones AO, Das IJ. Comparison of inhomogeneity correction algorithms in small photon fields. Med Phys 2005; 32:766–776.
18. Scott AJ, Nahum AE, Fenwick JD. Monte Carlo modeling of small photon fields: quantifying the impact of focal spot size on source occlusion and output factors, and exploring miniphantom design for small-field measurements. Med Phys 2009; 36:3132–3144.
19. Jones AO. A study of the dosimetry of small field photon beams used in intensity modulated radiation therapy in inhomogeneous media: Monte Carlo simulations, and algorithm comparisons and corrections. Med Phys 2004; 31:3161–3161.
20. Chow JCL, Leung MK, Van Dyk J. Variations of lung density and geometry on inhomogeneity correction algorithms: a Monte Carlo dosimetric evaluation. Med Phys 2009; 36:3619–3630.
21. Fogliata A, Vanetti E, Albers D, Brink C, Clivio A, Knöös T, Nicolini G, Cozzi L. On the dosimetric behaviour of photon dose calculation algorithms in the presence of simple geometric heterogeneities: comparison with Monte Carlo calculations. Phys Med Biol 2007; 52:1363–1385.
22. Krieger T, Sauer OA. Monte Carlo- versus pencil-beam-/collapsed-cone-dose calculation in a heterogeneous multilayer phantom. Phys Med Biol 2005; 50:859–868.
23. Nelson WR, Hirayama H, Rogers DWO. The EGS4 code system. SLAC Report 265, Stanford Linear Accelerator Center, Stanford, CA, 1965.

24. Kawrakow I, Rogers DWO. The EGSnrc code system: Monte Carlo simulation of electron and photon transport. NRCC Report PIPRS-701, National Research Council of Canada, Ottawa, 2000.
25. Rogers DW, Faddegon BA, Ding GX, Ma CM, We J, Mackie TR. BEAM: a Monte Carlo code to simulate radiotherapy treatment units. Med Phys 1995; 22:503–524.
26. Rogers DWO, Ma CM, Ding GX, Walters B, Sheikh-Bagheri D, Zhang GG. BEAMnrc users manual. NRC Report PIRS 509b(revF), 2001.
27. Ma CM, Reckwerdt P, Holmes M, Rogers DWO, Gesiser B. DOSXYZ user manual. NRC Report PIRS 509b, 1995.
28. Bielajew AF, Rogers DWO PRESTA-The Parameter Reduced Electron-step Transport Algorithm for electron Monte Carlo transport. Nucl Instrum Methods Phys Res B 1984; 18:535–548.
29. Chow JCL, Wong E, Chen JZ, Van Dyk J. Comparison of dose calculation algorithms with Monte Carlo methods for photon arcs. Med Phys 2003; 30:2686–2694.
30. Chow JCL, Grigorov GN, Jiang R. Improved peripheral dose calculation accuracy for a small MLC field brought by the latest commercial treatment planning system. J Radiother Practice 2006; 5:121–128.
31. Kim S, Liu CR, Zhu TC, Palta JR. Photon beam skin dose analyses for different clinical setups. Med Phys 1998; 25:860–866.
32. Ostwald PM, Kron T. Surface dose measurements for highly oblique electron beams. Med Phys 1996; 23:1413–1420.

https://doi.org/10.1017/S1460396910000427 Published online by Cambridge University Press